

Washington University School of Medicine

Digital Commons@Becker

2020-Current year OA Pubs

Open Access Publications

12-20-2022

A unique high-output cardiac hypertrophy phenotype arising from low systemic vascular resistance in Cantu syndrome

Gautam K Singh

Conor McClenaghan

Manish Aggarwal

Hongjie Gu

Maria S Remedi

See next page for additional authors

Follow this and additional works at: https://digitalcommons.wustl.edu/oa_4

 Part of the [Medicine and Health Sciences Commons](#)

Please let us know how this document benefits you.

Authors

Gautam K Singh, Conor McClenaghan, Manish Aggarwal, Hongjie Gu, Maria S Remedi, Dorothy K Grange, and Colin G Nichols

ORIGINAL RESEARCH

A Unique High-Output Cardiac Hypertrophy Phenotype Arising From Low Systemic Vascular Resistance in Cantu Syndrome

Gautam K. Singh, MD; Conor McClenaghan , PhD; Manish Aggarwal , MD; Hongjie Gu, MS; Maria S. Remedi , PhD; Dorothy K. Grange , MD; Colin G. Nichols , PhD

BACKGROUND: Cardiomegaly caused by left ventricular hypertrophy is a risk factor for development of congestive heart failure, classically associated with decreased systolic and/or diastolic ventricular function. Less attention has been given to the phenotype of left ventricular hypertrophy with enhanced ventricular function and increased cardiac output, which is potentially associated with high-output heart failure. Lack of recognition may pose diagnostic ambiguity and management complexities.

METHODS AND RESULTS: We sought to systematically characterize high-output cardiac hypertrophy in subjects with Cantu syndrome (CS), caused by gain-of-function variants in *ABCC9*, which encodes cardiovascular K_{ATP} (ATP-sensitive potassium) channel subunits. We studied the cardiovascular phenotype longitudinally in 31 subjects with CS with confirmed *ABCC9* variants (median [interquartile range] age 8 years [3–32 years], body mass index 19.9 [16.5–22.9], 16 male subjects). Subjects with CS presented with significant left ventricular hypertrophy (left ventricular mass index 86.7 [57.7–103.0] g/m² in CS, n=30; 26.6 [24.1–32.8] g/m² in controls, n=17; $P<0.0001$) and low blood pressure (systolic 94.5 [90–103] mmHg in CS, n=17; 109 [98–115] mmHg in controls, n=17; $P=0.0301$; diastolic 60 [56–66] mmHg in CS, n=17; 69 [65–72] mmHg in control, n=17; $P=0.0063$). Most (21/31) subjects with CS exhibited eccentric hypertrophy with normal left ventricular wall thickness. Congestive heart failure symptoms were evident in 4 of the 5 subjects with CS aged >40 years on long-term follow-up.

CONCLUSIONS: The data define the natural history of high-output cardiac hypertrophy resulting from decreased systemic vascular resistance in subjects with CS, a defining population for long-term consequences of high-output hypertrophy caused by low systemic vascular resistance, and the potential for progression to high-output heart failure.

Key Words: *ABCC9* ■ cardiomegaly ■ echocardiography ■ heart failure ■ high-output state

Left ventricular hypertrophy (LVH) without structural disorder of the heart represents a risk factor for development of heart failure (HF).¹ Initially, LVH may serve to maintain contractile forces and counteract increased ventricular wall stress caused by altered loading conditions. However, increased wall stress may lead to apoptosis, myocardial fibrosis, and architectural changes that are associated with decline in systolic reserve capacity and diastolic function.² Thus, LVH serves as a risk factor and structural prerequisite for the development of HF from impaired pump function that can progress to left ventricular (LV) remodeling without

symptoms of HF and then to symptomatic congestive HF, a low-output state. This current clinical HF paradigm of an LVH phenotype with impaired pump function and low cardiac output (CO) is predominantly cardiomyocentric. In current clinical practice, this essentially excludes primary vasculopathies that may be involved in the HF pathogenesis, including any LVH that may be related to a primary vascular pathology with the potential to progress to congestive HF. Relatively little is understood about the underlying mechanisms and natural history of high-output cardiac hypertrophy states arising from primary vascular pathology. Such lack of awareness could

Correspondence to: Gautam K. Singh, MD, Central Michigan University School of Medicine, Children's Hospital of Michigan, Carls Building, 3901 Beaubien Street, Detroit, MI 48201. Email: gsingh3@dmc.org; Colin G. Nichols, PhD, Washington University in St. Louis, Department of Cell Biology and Physiology, 660 South Euclid Avenue, St. Louis, MO 63110. Email: cnichols@wustl.edu

For Sources of Funding and Disclosures, see page 11.

© 2022 The Authors. Published on behalf of the American Heart Association, Inc., by Wiley. This is an open access article under the terms of the [Creative Commons Attribution](https://creativecommons.org/licenses/by/4.0/) License, which permits use, distribution and reproduction in any medium, provided the original work is properly cited.

JAHA is available at: www.ahajournals.org/journal/jaha

CLINICAL PERSPECTIVE

What Is New?

- Cantu syndrome (CS) is characterized by a high-output state that may progress to heart failure with normal diastolic function, low systemic vascular resistance, and high output.
- Although CS and heart failure with preserved ejection fraction share the general symptoms of heart failure, they are distinct in cardiac phenotype and pathophysiology, and CS should be considered in the differential diagnosis of heart failure where ventricular systolic function appears normal, such as heart failure with preserved ejection fraction.

What Are the Clinical Implications?

- Because of a current lack of awareness of CS complications, many subjects with CS have been misdiagnosed with hypertrophic cardiomyopathy or dilated cardiomyopathy, and as a result have been administered conventional therapies including angiotensin-converting enzyme inhibitors, β -blockers, or sildenafil, but treatment with these agents is based on heart failure paradigms that do not take into account low systemic vascular resistance states and may exacerbate the underlying primary decrease in systemic vascular resistance and hence worsen symptoms.

Nonstandard Abbreviations and Acronyms

| | |
|------------------------|---------------------------------------|
| CO | cardiac output |
| CS | Cantu syndrome |
| HR | heart rate |
| ICSR | International Cantu Syndrome Registry |
| K_{ATP} | ATP-sensitive potassium |
| LVMI | left ventricular mass index |
| PAAT | pulmonary artery acceleration time |
| RWT | relative wall thickness |

result in ambiguity of clinical diagnosis, adversely influencing clinical screening and management.

We describe the natural history of a cardiac phenotype characterized by LVH with enhanced ventricular function and high-output state caused by genetically determined vasodilatation, in a cohort of subjects with Cantu syndrome (CS; Online Mendelian Inheritance in Man number 239850), an autosomal dominant condition caused by gain-of-function variants in *ABCC9* and, less commonly, in *KCNJ8*, which encode the regulatory (Sulfonylurea receptor 2 [SUR2]) and pore-forming (inwardly rectifying potassium channel family member 6.1)

subunits, respectively, of K_{ATP} (ATP-sensitive potassium) channels.^{3–6} Subjects with CS exhibit a wide constellation of clinical features,^{7–9} with congenital hypertrichosis, osteochondrodysplasia, and characteristic facies. We describe the longitudinal cardiovascular phenotype in 31 subjects with CS and discuss the potential mechanistic basis, natural history of the high-output state, and the clinical implications of this sentinel example of high-output cardiac hypertrophy associated with primary decreased systemic vascular resistance.

METHODS

Study Design and Data Collection

We studied the cardiovascular phenotype in 31 subjects with CS with confirmed *ABCC9* variants.⁹ All subjects were enrolled in the ICSR (International Cantu Syndrome Registry), established as an international multicenter Research electronic data capture-based registry to collate systematic clinical and genetic data on subjects with CS. Longitudinal data were collected during annual CS research clinics over 7 years from 2013 to 2019.⁹ Initial cardiovascular findings in the first 11 subjects with CS studied in the Washington University clinic have been reported previously.^{10,11} Cardiovascular phenotype in 17 age- and sex-matched normal healthy subjects were included as controls. Medical history and prior medical records, including results of molecular genetic testing, were collated in questionnaire form for each subject, either during routine visits as part of standard care or during the annual CS research clinic. All studies were approved by the Washington University School of Medicine Institutional Review Board of the Human Research Protection Office and performed at St. Louis Children's Hospital. All data were collected after informed consent of the subjects or of the parents or legal guardians for subjects aged <18 years. The data that support the findings of this study are available from the corresponding authors upon reasonable request.

Cardiovascular Examination

Cardiovascular examination included detailed history, tracking of symptoms, complete physical examination, and standard vital measurements.

Blood Pressure

Blood pressure (BP) and heart rate (HR) were measured 3 times by manual sphygmomanometer with appropriate cuff size, in the resting supine position, and after 2 and 5 minutes in the upright position, consistent with American Academy of Pediatrics guidelines,¹² to ascertain orthostatic vital sign changes. BP measurements were compared with published normative values by sex and age (www.nhlbi.nih.gov/files/docs/guidelines/child_tbl.pdf).

Cardiac Structure

Transthoracic complete echocardiographic examinations were performed according to American Society of Echocardiography guidelines (Vivid 9 and E95; General Electric Medical Systems). M-mode measured LV end-diastolic diameter, LV end-systolic diameter, and end-diastolic posterior wall thickness were used to calculate relative wall thickness (relative wall thickness (RWT)=2×posterior wall thickness/LV end-diastolic diameter)¹³ and LV mass. LV mass index (LVMI) was calculated and indexed to height using the Devereux equation.¹⁴ To define ventricular structural phenotype, the 95th percentiles for LVMI for children older than 9 years (>40g/m^{2.7} in female children and >45g/m^{2.7} in male children) and the 95th percentile value for RWT for normal children and adolescents (RWT>0.41) were used as cutoff values to categorize abnormal LV geometry.^{15,16} Subjects with LVMI and RWT below the 95th percentile were categorized as having normal LV geometry. Concentric remodeling was defined as normal LVMI and elevated RWT, eccentric hypertrophy as elevated LVMI and normal RWT, and concentric hypertrophy as elevated LVMI and RWT.¹⁷ Right ventricular (RV) dimensions in apical 4-chamber images were measured for basal and midcavity minor axis and longitudinal axis in RV focus view.

Cardiac Function

LV systolic function was measured in standard format using M-mode imaging for LV fractional shortening and the 2-dimensional imaging modified Simpson method for LV ejection fraction. Myocardial mechanics were evaluated by measurement of strain (dimensionless measure of myocardial deformation) and strain rate (time derivative of strain), which correlates with LV peak elastance, reflecting contractile performance.¹⁸ LV peak global longitudinal strain, strain rates, early diastolic global longitudinal strain rates, and late diastolic global longitudinal strain rates were measured using 2-dimensional speckle-tracking echocardiography (EchoPAC, General Electric Medical Systems). LV and RV systolic and diastolic functions were also evaluated using tissue Doppler imaging.¹⁹ Tissue Doppler imaging–measured indices were compared with the normal controls and with published normative values by sex and age.²⁰

Cardiovascular Hemodynamics

CO was calculated from measured aortic valve annular diameter, time velocity integral of pulse-wave Doppler velocity in LV outflow tract, and HR (beats per minute) using the equation $CO = \pi \times (\text{diameter}/2)^2 \times \text{time velocity integral} \times \text{HR} \times 100$ (liters per minute), and indexed (cardiac index) against body surface area (liters per minute per square meter). Systemic vascular resistance (SVR) was calculated by the formula: $SVR = \text{mean}$

arterial pressure/CO (mean arterial pressure [systolic BP+{2×diastolic BP}/3] and CO (millimeters of mercury per minute per milliliter). Additionally, cardiac hemodynamics were studied in 5 subjects with CS by cardiac catheterization, in 2 subjects when they had either device closure (CS001) or before surgical ligation (CS005) of a patent ductus arteriosus (PDA), and in another 3 subjects who underwent cardiac catheterization for hemodynamic study (CS002 and CS004) or interventional embolization of a major aorto-pulmonary collateral (CS020) as a part of standard of care.

Pulmonary Hemodynamics

Pulmonary artery acceleration time (PAAT) demonstrates a strong, inverse correlation with invasively measured pulmonary hemodynamics.^{21,22} We obtained PAAT using pulse Doppler velocity, as previously reported, and standardized against HR with the ratio of PAAT/RV ejection time.²³

Vascular Properties

M-mode ultrasonography of the ascending aorta was used to assess arterial stiffness using the modified equation for calculation of Young's elastic modulus: Young's elastic modulus=(aortic radius in systole/arterial wall thickness)×(pulse pressure×fractional change in diameter of the aorta from end-diastole to end-systole).²⁴

Statistical Analysis

Data were analyzed by SAS version 9.4 (SAS Institute, Cary, NC). Quantitative data are presented as median (interquartile range), and qualitative data are presented as number (percent). In case–control comparisons, only values from the first clinic visit of each individual are included. A Wilcoxon rank sum test was used to assess differences between nonnormal or continuous variables of unknown distributions between groups. χ^2 test or Fisher exact test (if the number for any group was <5) was used to test associations between categorical factors and groups. In longitudinal analysis, only subjects who had at least 2 visits were included. A mixed random-effects repeated measures model was performed to describe the rate of change of continuous variables versus time. $P < 0.05$ was considered as significant.

RESULTS

Demographic and Anthropometric Characteristics of the CS Cohort

Cardiovascular phenotype was initially assessed in 31 subjects with CS aged 1 to 69 years. The majority (20/31; 65%) were aged <18 years at the initial enrollment or evaluation for standard of care, and 16 (52%)

were male subjects. The control group was similar in age, sex, race, and ethnicity distribution (Table 1). Anthropometric data were not significantly different between the 2 groups, except height, where the subjects with CS were shorter (Table 1).

Cardiovascular Phenotype in CS Subjects

All subjects with CS had normal cardiac segmental anatomy, and they had normal wall thickness on average, but all exhibited markedly enlarged hearts and LV volumes and mass (LVMI) throughout the course of the investigation, compared with normal controls (Figure 1A through 1D). The majority (21/31; 68%) of subjects were determined to exhibit eccentric hypertrophy with normal LV posterior wall thickness, despite increased LVMI (Table 2). A further 6 subjects (6/31; 19%) who exhibited concentric hypertrophy with increased LVMI and increased wall thickness (Table 2) were predominantly younger (all aged <18 years at presentation).

Subjects with CS demonstrated enhanced LV fractional shortening (Figure 2A) and ejection fraction (Figure 2B). In addition, LV contractility was significantly increased, with elevated LV global longitudinal systolic strain (Figure 2C) and systolic strain rate (Figure 2D). LV global longitudinal diastolic strain rate was marginally increased, and myocardial velocity indices were proportionally altered (Figure 2E and 2F, Table 2).

Because of the limited availability of RV-focused 4-chamber images, RV dimensions were only measurable in 15 of 31 subjects with CS and 10 of 17 control subjects. There was no significant difference ($P=0.19$)

between the subjects with CS and the controls in median and quartile RV basal (2.8 cm; 2.5–3.9 cm versus 3.0 cm, 2.8–3.9 cm) and mid (1.8 cm; 1.5–2.5 cm versus 2.0 cm, 1.8–2.9 cm) axes, and longitudinal axis (4.8 cm; 4.5–7.2 cm versus 5.2 cm, 5.0–7.5 cm). The median RV annular systolic velocity S' in subjects with CS were similar to those in the controls (12 cm/s versus 11.5 cm/s).

Hemodynamics: High CO With Low Systemic Vascular Resistance

Subjects with CS consistently exhibited significantly higher cardiac indices and decreased peripheral systemic vascular resistance than controls, and this was associated with significantly increased vascular compliance and diminished vascular tone (Figure 3, Table 2). Five subjects who were additionally assessed by cardiac catheterization (CS001, CS002, CS004, CS005, and CS020) displayed further evidence of high CO (cardiac index of 5.2–8.75 L/min⁻¹ per m⁻², respectively), with normal Left ventricular end diastolic pressure (7–9 mmHg) and capillary wedge pressure (9–11 mmHg). Systemic BP in individuals with CS assessed during the clinic (age range, 3–48 years) were low (Table 2) despite elevated CO, consistent with markedly decreased SVR and increased vascular compliance. Despite this, no subjects demonstrated HR or BP changes on standing.

Pulmonary Hemodynamics

PAAT and PAAT/RV ejection time were in the normal range (>115 ms and 0.35 in adults, $n=12$; and >95 ms

Table 1. Demographic and Clinical Characteristics for Control and Case Individuals

| | Control | Case | P value |
|---|--------------------------|------------------------|---------|
| Demographics | | | |
| Men, n (%) [N] | 10 (58.82) [17] | 16 (51.6) [31] | 0.6316 |
| Median age at the first visit, y, (IQR) [N] | 15 (14–17) [17] | 8 (3–32) [31] | 0.4101 |
| Race, n (%) | | | |
| White | 15 (88.24) | 30 (96.8) | 0.1258 |
| Black | 2 (11.76) | 0 (0) | |
| Not recorded | 0 (0) | 1 (3.2) | |
| Ethnicity, n (%) | | | |
| Hispanic or Latino | 0 (0) | 8 (25.8) | 0.1638 |
| Non-Hispanic or Latino | 8 (47.1) | 22 (71.0) | |
| Not recorded | 9 (52.9) | 1 (3.2) | |
| Anthropometrics | | | |
| Median BMI (IQR) [N] | 19.6 (18.1–20.4) [17] | 19.9 (16.5–22.9) [30] | 0.6363 |
| Median weight, kg (IQR) [N] | 53.3 (48.4–61.4) [17] | 35.2 (18.9–60) [30] | 0.2055 |
| Median height, cm (IQR) [N] | 166.8 (158.8–172.2) [17] | 137.5 (102.3–162) [30] | 0.0169 |
| Median BSA (Du Bois) (IQR) [N] | 1.62 (1.5–1.7) [17] | 1.1 (0.7–1.7) [30] | 0.1013 |

Quantitative data are presented as median (IQR), and qualitative data are presented as n (%). P values are from Wilcoxon rank sum test for continuous variables, or χ^2 test or Fisher exact test (if any expected cell number <5) for categorical variables. $P<0.05$ indicates there is a significant difference between case and control. BMI indicates body mass index; BSA, body surface area; and IQR, interquartile range.

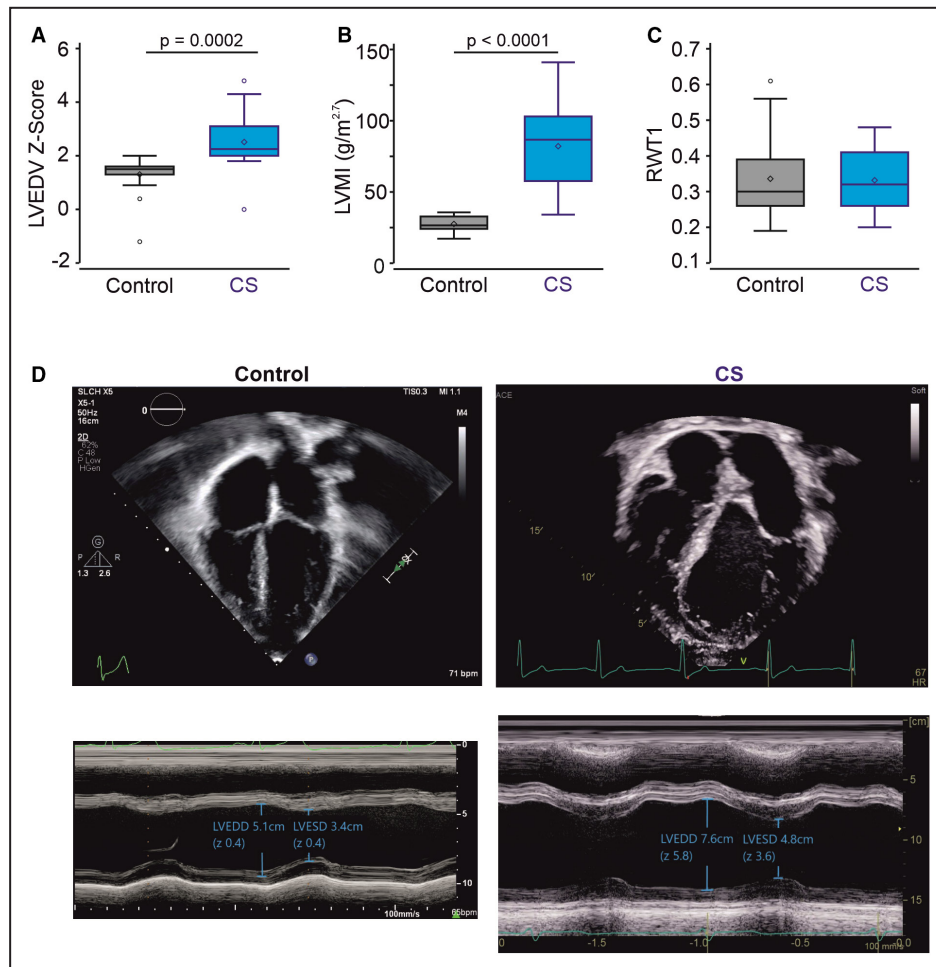


Figure 1. Structural remodeling in the CS heart.

LVEDV Z score (A) and LVMI (B) are increased in subjects with CS compared with the control group. C, RWT1 is normal in subjects with CS. P values from Wilcoxon rank sum tests are shown. $P < 0.05$ indicates a statistically significant difference between control and CS cohorts. D, Representative 4C (above) and M-mode (below) echocardiographic images of a control (male sex, 64 kg, ages 15 years [left]) and CS (male sex, 77 kg, aged 16 years [right]) subjects. 4C end-diastolic volumes were 116 mL ($Z = -0.5$) and 389 mL ($Z = 8.1$), and ejection fractions were 59% and 70%, for the control and subject with CS, respectively. M-mode dimensions were diastolic 5.1 cm ($Z = 0.4$) and 7.6 cm ($Z = 5.8$), systolic 3.4 cm ($Z = 0.4$) and 4.8 cm ($Z = 3.6$), and shortening fraction was 33% and 37%, respectively. CS indicates Cantu syndrome; LVEDD, left ventricular end diastolic dimension; LVEDV, left ventricular end-diastolic volume; LVESD, left ventricular end systolic dimension; LVMI, left ventricular mass index; and RWT1, relative wall thickness.

and 0.42 in children, $n = 19$, respectively), suggestive of normal pulmonary systolic pressure and vascular resistance at initial presentation and during follow-up.

Characteristic Abnormalities of Valves and Great Vessels: Aortic Ectasia and Aortic Regurgitation

Almost all CS individuals (29/31, 94%) had aortic ectasia with dilation of the aortic root (Z score, 3.22–3.98) and ascending aorta (Z score, 2.16–3.57) at the first visit. In the remaining 2 subjects, aortic root dilation developed within 2 years follow-up. No subjects with CS reached aortic dimension ≥ 5 cm, a cutoff point used for surgical

aortic graft replacement in subjects with connective tissue disorders such as Marfan syndrome. Trivial or mild, and hemodynamically nonsignificant, aortic regurgitation was observed in some subjects, but there was no evidence of progression during the course of follow-up. This was not associated with abnormal valve anatomy but was associated with aortic root dilation > 3 Z score.

Features of Fetal Circulation

Fifteen of 31 subjects with CS (48%) of all ages had features of fetal circulation that persisted, including small aorto-pulmonary bronchial arteries in the thorax that were evident by color-flow Doppler mapping. The

Table 2. Cardiac Function and Hemodynamics

| | Control | Case | P value |
|--|-----------------------------|-----------------------------|---------|
| LV structure and function | | | |
| Median LVEDV, mL, (IQR) [N] | 91 (78 to 98) [17] | 84.3 (53.3 to 165) [31] | 0.066 |
| Median Z score of LVEDV (IQR) [N] | 1.5 (1.3 to 1.6) [17] | 2.3 (2.0 to 3.1) [31] | <0.0001 |
| Median LVDd, cm, (IQR) [N] | 4.3 (4.0 to 4.5) [17] | 4.4 (3.9 to 5.6) [31] | 0.2172 |
| Median Z score of LVDd (IQR) [N] | 1.20 (0.90 to 1.80) [17] | 2.4 (1.9 to 3.3) [31] | <0.0001 |
| Median LVMI-M-mODE, g/m ^{2.7} , (IQR) [N] | 26.6 (24.1 to 32.8) [17] | 86.7 (57.7 to 103.0) [30] | <0.0001 |
| LVMI abnormal, n (%) | | | <0.0001 |
| Normal | 17 (100) | 3 (9.7) | |
| Abnormal | 0 (0) | 26 (83.8) | |
| Not recorded | 0 (0) | 2 (6.5) | |
| Remodeling, n (%) | | | |
| Normal | 14 (82.3) | 2 (6.5) | <0.0001 |
| Concentric remodeling | 3 (17.7) | 6 (19.3) | |
| Eccentric hypertrophy | 0 (0) | 21 (67.7) | |
| Not recorded | 0 (0) | 2 (6.5) | |
| Median RWT1 (IQR) [N] | 0.3 (0.26 to 0.39) [17] | 0.32 (0.26 to 0.41) [31] | 0.9035 |
| RWT1 abnormal, n (%) | 3 (17.7) | 7 (21.2) | 0.7271 |
| Median FS, %, (IQR) [N] | 36 (36 to 38) [17] | 43.4 (40.4 to 46.6) [31] | <0.0001 |
| FS abnormal, n (%) | 0 (0) | 11 (33.3) | 0.0038 |
| Median LV GS long, % overall, (IQR) [N] | -18.0 (-20.1 to -17.1) [17] | -24.3 (-25.4 to -23.1) [30] | <0.0001 |
| LV GS long, % overall abnormal, n (%) | 8 (47.1) | 29 (87.9) | <0.0001 |
| Median LV GSRs long, %/s (IQR) [N] | -1.0 (-1.1 to -0.9) [17] | -1.4 (-1.7 to -1.3) [22] | 0.0001 |
| Median LV GSRe long, %/s (IQR) [N] | 1.6 (1.4 to 1.9) [17] | 2.0 (1.7 to 2.5) [22] | 0.0035 |
| Median LV GS Ra long, %/s (IQR) [N] | 0.55 (0.48 to 0.82) [17] | 0.87 (0.70 to 1.7) [22] | 0.0025 |
| Median LV E'/A', (IQR) [N] | 2.9 (2.6 to 3.2) [17] | 2.0 (1.7 to 2.5) [28] | 0.0050 |
| Median LV E'/E', (IQR) [N] | 6.3 (5.3 to 8.0) [17] | 7.9 (6.0 to 9.0) [30] | 0.1273 |
| LV E'/E' abnormal, n (%) | | | |
| Normal | 10 (58.8) | 15 (48.4) | 0.2197 |
| Borderline | 4 (23.5) | 14 (45.2) | |
| Abnormal | 0 (0) | 0 (0) | |
| Not recorded | 3 (17.7) | 2 (6.5) | |
| Median LV MPI (IQR) [N] | 0.35 (0.32 to 0.38) [17] | 0.37 (0.32 to 0.40) [30] | 0.9897 |
| LV MPI abnormal, n (%) | 11 (64.7) | 25 (75.8) | 0.6646 |
| Hemodynamics | | | |
| Median EF, %, (IQR) [N] | 63 (59 to 65) [17] | 68.5 (61 to 76) [31] | 0.0124 |
| EF abnormal, n (%) | 4 (25.5) | 20 (60.6) | 0.0045 |
| Median CI, L/min per m ² , (IQR) [N] | 4.20 (4 to 4.8) [17] | 6.7 (5.5 to 7.6) [31] | 0.0004 |
| CI abnormal, n (%) | 0 (0) | 25 (75.8) | <0.0001 |
| Median Young's elastic modulus, (IQR) [N] | 14.8 (10.8 to 18.5) [17] | 26.1 (16.6 to 43.4) [25] | 0.0043 |
| Median systolic pressure, mmHg, (IQR) [N] | 109 (98 to 115) [17] | 94.5 (90 to 103) [17] | 0.0301 |
| Median diastolic pressure, mmHg, (IQR) [N] | 69 (65 to 72) [17] | 60 (56 to 66) [17] | 0.0063 |
| Median systemic vascular resistance, (IQR) [N] | 20 (18.8 to 21.1) [17] | 9.5 (9.1 to 11.2) [17] | <0.0001 |
| Median systolic AAO dimension, cm, (IQR) [N] | 2.7 (2.5 to 2.8) [17] | 2.3 (1.8 to 3.2) [29] | 0.4841 |

(Continued)

Table 2. Continued

| | Control | Case | P value |
|---|-----------------------|-----------------------|---------|
| Median Z score of systolic AAO dimension, (IQR) [N] | 1.6 (1.3 to 1.8) [17] | 2.9 (2.2 to 3.8) [29] | <0.0001 |
| Median diastolic AAO dimension, cm, (IQR) [N] | 2.5 (2.4 to 2.7) [17] | 2.0 (1.5 to 2.8) [17] | 0.2752 |
| Median heart rate, bpm, (IQR) [N] | 77 (72 to 89) [17] | 93 (78 to 110) [31] | 0.0317 |

Quantitative data are presented as median (IQR), and qualitative data are presented as n (%). P values are from Wilcoxon rank sum test for continuous variables, or χ^2 test or Fisher exact test (if any expected cell number <5) for categorical variables. For other variables, P values were associated with mixed general linear model for longitudinal data analysis. $P < 0.05$ indicates there is a significant difference between case and control. AAO indicates ascending aorta; CI, cardiac index; E'A', early diastolic velocity of mitral annulus (E') over late diastolic velocity of mitral annulus (A'); E/E', early mitral peak inflow velocity (E) over early diastolic velocity of mitral annulus (E'); EF, ejection fraction; FS, fractional shortening; IQR, interquartile range; LV, left ventricular; LV GS long, left ventricular global longitudinal strain; LV GSRe, left ventricular global peak late diastolic strain rate; LV GSRe, left ventricular global peak early diastolic strain rate; LV GSrs, left ventricular systolic global strain rate; LV MPI, left ventricular myocardial performance index; LVDd, left ventricular diastolic dimension; LVEDV, left ventricular end-diastolic volume; LVMI, left ventricular mass index; LVMI-M-mode, left ventricular mass index (as determined by M-mode echocardiography); and RWT1, relative wall thickness.

most clinically pertinent feature of fetal circulation was the PDA present in 9 of 31 (29%) subjects with CS persistent beyond 2 months of age.

Pericardial Effusion Complicating Clinical Course

Six of 31 subjects with CS (19%) had a pericardial effusion. A mother (CS004) and her daughter (CS002) developed pericardial effusion before the age 19 years and 9 years, whereas the 4 other subjects (CS011, CS016, CS021, and CS037) developed pericardial effusion in adulthood.

Electrocardiographic Monitoring

ECGs (n=31) revealed first-degree atrioventricular block in 6 subjects, fascicular block in 2 subjects, and T-wave axis abnormalities in inferior leads in 8 subjects, but there was no evidence of QT shortening or corrected QT prolongation, nor of atrial or ventricular arrhythmia. None of the subjects with CS met the voltage criteria for RV hypertrophy or LVH.

Natural History

Four of 31 subjects with CS have been followed longitudinally from early childhood (CS001, CS002, CS003,

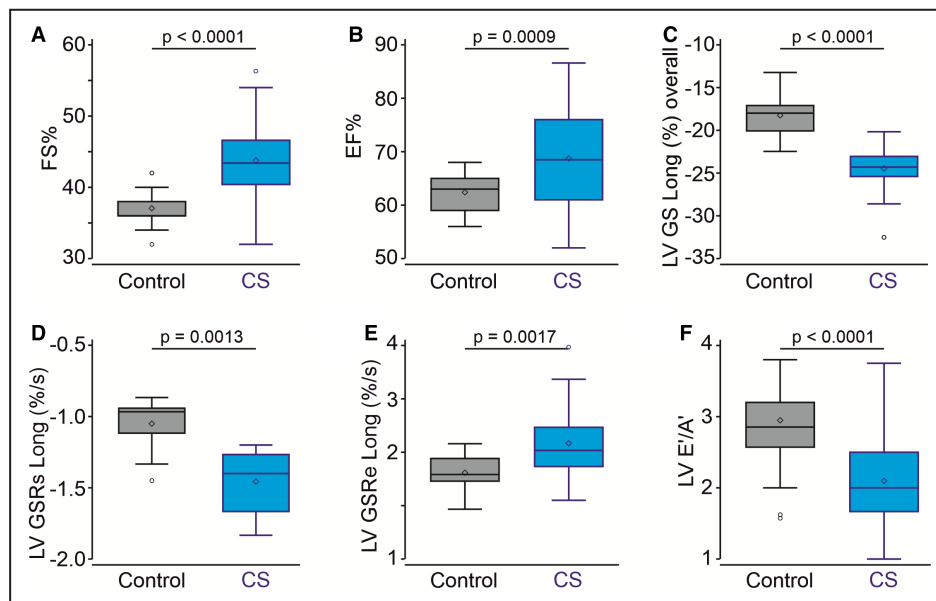


Figure 2. Enhanced left ventricular function in CS.

Left ventricular FS (%) (A) and EF (%) (B) are increased in subjects with CS compared with the control group. LV GS Long overall (C), LV GSrs Long (D), and LV GSRe Long (E) are increased in subjects with CS. F, E'/A' is decreased in subjects with CS. P values from Wilcoxon rank sum tests are shown. $P < 0.05$ indicates a statistically significant difference between the control and CS cohorts. A' indicates late diastolic velocity of mitral annulus; CS, Cantu syndrome; E', early diastolic velocity of mitral annulus; E'/A', ratio of E' over A'; EF, ejection fraction; FS, fractional shortening; LV, left ventricle; LV GS Long overall, LV global longitudinal systolic strain; LV GSRe Long, LV diastolic global strain rate; and LV GSrs Long, LV systolic global strain rate.

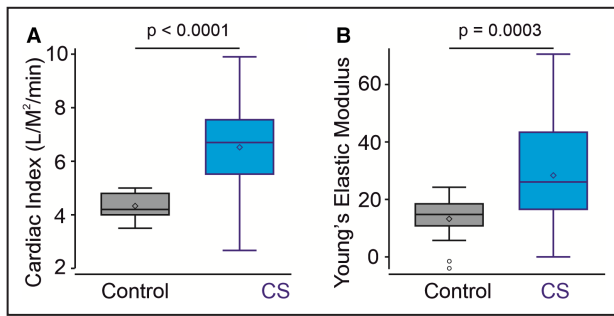


Figure 3. Hemodynamic metrics in subjects with CS. Cardiac index (cardiac output normalized to body surface area) (A) and vascular compliance (as measured by Young's elastic modulus) (B) are increased in subjects with CS. *P* values from Wilcoxon rank sum tests are shown. *P* < 0.05 indicates a statistically significant difference between the control and CS cohorts. CS indicates Cantu syndrome.

and CS005) and 1 from early adulthood (CS004) through routine clinical assessments as a part of standard of care for a median of 9 years before systematic follow-up in the CS research clinic over the ensuing 7 years. The other 26 subjects with CS were studied longitudinally in the CS research clinic for a median of 3 years (range, 2–7 years).

Cardiac Structure and Function

LV size increased gradually in all subjects with CS (Figure 4A) but more significantly in children and teenagers (Figure 4B and 4C). For the whole cohort, enhanced LV systolic function (ejection fraction; Figure 5A) and contractility (LV global longitudinal strain; Figure 5B) remained relatively stable over 7 years of follow-up.

Hemodynamics

The abnormally high vascular compliance remained relatively unchanged over time (Figure 5C). Overall, systemic vascular resistance remained low, and cardiac index remained high for the whole cohort during follow-up period. The majority of subjects with CS remained in New York Heart Association functional class I, although 4 of 31 (CS004, CS021, CS035, and CS022), representing 4 of the 5 women aged ≥ 40 years, exhibited evidence of symptomatic HF. CS004 developed fatigue, shortness of breath on climbing stairs, and orthopnea (New York Heart Association functional class III) at the age of 42 years and before the onset of atrial fibrillation, which worsened the HF severity (brain natriuretic peptide, 200 pg/mL). Treatment with an angiotensin-converting enzyme inhibitors, prescribed by her treating cardiologist at the time for HF management, exacerbated symptoms, and was later discontinued. The 3 other subjects (CS021, CS035, and CS022) developed HF (all New York Heart Association functional class II) at age 46, 58, and 69 years, respectively, with increasing symptoms of fatigue, orthopnea,

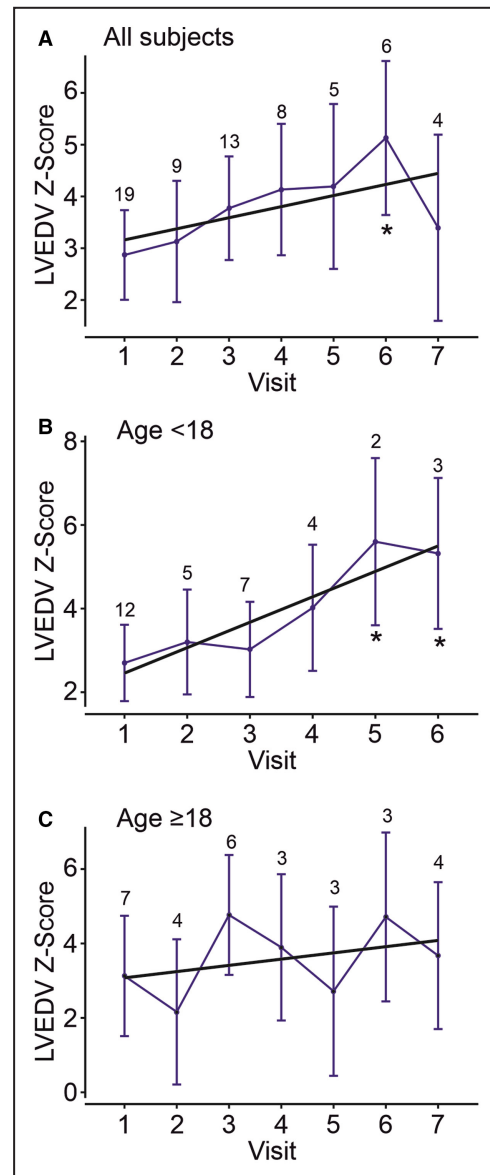


Figure 4. Longitudinal assessment of left ventricle dimension.

LVEDV Z score was determined in the cohort of subjects with CS over up to 7 years. A trend toward increasing LVEDV Z scores was observed for all subjects with CS (A), and this was more pronounced for younger subjects (first visit at age <18 years [B]) than older subjects (first visit at age >18 years [C]). Data are shown as median Z score value for the CS cohort per visit (blue circles with 95% CIs; linear regression fits in black; slope=0.26, *P*=0.0609 [A]; slope=0.39, *P*=0.0208 [B]; slope=0.15, *P*=0.3652 [C]). Number of subjects at each visit is shown above data points. Data were fit with a mixed random-effects repeated measures model to test whether changes across time were significant. **P* < 0.05 for any visit compared with visit 1. CS indicates Cantu syndrome; LV, left ventricular; and LVEDV, left ventricular end diastolic volume.

and exercise intolerance, and were treated with mild diuretics. Although all other subjects with CS were in New York Heart Association functional class I, they generally complained of fatigue and intolerance to

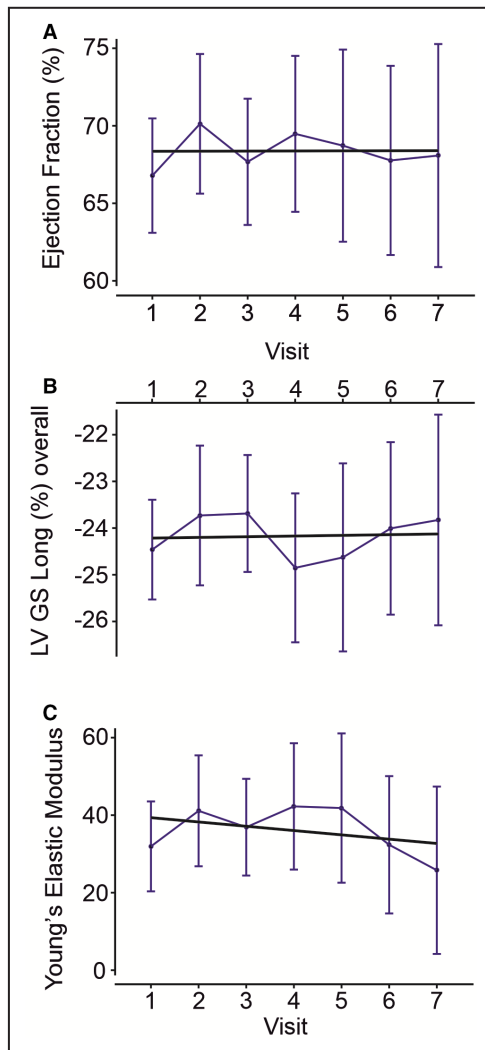


Figure 5. Longitudinal assessment of ventricular function and vascular elasticity.

A and B, Both left ventricular ejection fraction (**A**) and LV GS Long overall (**B**) remained stable over repeated annual visits for subjects with CS. Number of subjects included in each repeat visit is indicated. Data are shown as median Z score value for the CS cohort per visit (blue circles with 95% CIs; linear regression fit shown in black; slope=−0.85, $P=0.06$ [**A**]; slope=0.14, $P=0.34$ [**B**]). **C,** Young's elastic modulus did not significantly change over repeated annual visits for subjects with CS. Data are shown as median Z score value for the CS cohort per visit (blue circles with 95% CIs; linear regression fit shown in black; slope=−0.25, $P=0.8755$). Data were fit with a mixed random-effects repeated measures model that showed there were no statistically significant differences in values over time. CS indicates Cantu syndrome; LV, left ventricular; and LV GS, left ventricular systolic global strain rate.

moderate- or high-intensity exercise. Three additional subjects (CS005, CS006, and CS0020, aged 23, 17, and 20 years, respectively) had orthopnea, but became symptom free after they were taken off an angiotensin-converting enzyme inhibitor that was prescribed by their treating physicians because of cardiomegaly.

Pericardial Effusion

One mother (CS004) and her daughter (CS002) developed hemodynamically significant recurrent pericardial effusion at 19 years and 9 years of age, respectively, that required repeated pericardiocentesis and ultimately pericardial stripping. The pericardial fluid had an elevated protein concentration (4.7 g/dL and 4.4 g/dL), normal glucose (90 mg/dL and 95 mg/dL), and predominant lymphocyte population on cell count ($\approx 70\%$) in the presence of negative inflammatory markers (erythrocyte sedimentation rate <10 mm/h, C-reactive peptide <0.1 mg/L, negative serum antiextractable nuclear antigen antibody, and normal C3 and C4 complements), suggesting that the effusion might be lymphatic pericardial fluid. Four other subjects (CS011, CS016, CS021, and CS037) had stable and asymptomatic mild-to-moderate pericardial effusion during follow-up.

Features of Fetal Circulation

Subjects with CS with aorto-pulmonary collaterals were asymptomatic, except for 1 subject (CS020, aged 20 years) with a large aorto-pulmonary bronchial artery who developed hemoptysis and required embolization of the vessel by cardiac catheterization. Compared with preintervention, the postintervention follow-up Z score of left ventricular end diastolic volume indexed (2.8 versus 2.7), and left ventricular end diastolic dimension (2.5 versus 2.4) as well as LVMI (88 versus 86 g/h^{2.7}) and cardiac index (6.5 versus 6.9 L/min per m²) were relatively unchanged. In 9 subjects with persistent PDA beyond 2 months of age, 6 had a hemodynamically significant shunt requiring surgical or device closure before 1 year of age, and before their enrollment in the study. They all had enlarged left ventricles (LV end-diastolic volume Z score, 2.9–3.3) and increased cardiac index (6.7–7.5 L/min per m²) even a median of 3 years (range, 2–7 years) after the closure of the PDA. Taken together, in these subjects with CS, increased CO, and enlarged left ventricle were predominantly associated with low SVR and high output.

DISCUSSION

We describe a specific cardiovascular phenotype resulting from gain-of-function variants in *ABCC9* (*SUR2*) that presents with dilated left ventricle with increased LV mass, but increased contractility and high CO, associated with genetically determined primary low systemic vascular resistance. Although *SUR2* proteins are regulatory subunits of both cardiac and vascular smooth muscle K_{ATP} channels,²⁵ we see no evidence of cardiac arrhythmias, and essentially none were observed during 24 hours of ambulatory ECG monitoring in a previous study.¹⁰ That study revealed generally high HR for age that failed to lower appropriately

during sleeping hours, suggesting a relatively elevated sympathetic activity but diminished vagal activity. Mechanistic studies in mouse models of CS, in which CS variants in *ABCC9* and *KCNJ8* were engineered into the equivalent mouse loci using CRISPR/Cas9, indicate that cardiac enlargement and enhanced CO are responses to decreased vascular resistance arising from the vascular smooth muscle K_{ATP} channel gain-of-function, because cardiac enlargement can be reversed when vascular K_{ATP} channels specifically are inhibited or genetically knocked down^{26,27} (Figure 6). Thus, the cardiac hypertrophy and high-output state in CS may be a consideration for causes of HF but are distinct in phenotype, hemodynamic, and natural history from cardiomyopathies of known causes, including HF with preserved ejection fraction.

The CS phenotype is distinct from dilated cardiomyopathy, in which the ventricles are enlarged but thin walled, and systolic function is decreased, and from hypertrophic cardiomyopathy, in which ventricular walls are thickened but chamber cavity is either normal or smaller than normal. Unlike CS, both dilated cardiomyopathy and hypertrophic cardiomyopathy may have abnormal diastolic indexes of LV filling and diastolic function.²⁸ Systematic evaluation of CS cardiovascular features has previously been lacking, and the combination of dysmorphic features and cardiomegaly has previously led to misdiagnoses of subjects with CS as having a metabolic storage disorder or other genetic syndrome, or dilated cardiomyopathy or hypertrophic cardiomyopathy, leading to inappropriate and potentially harmful therapeutic choices. CS is also distinct from other high-output conditions in which low SVR is secondary to the underlying cause. For example, high-output cardiac failure associated with the hyperdynamic phase of sepsis is mainly driven by inflammatory cytokines, which cause systemic vasodilation in the setting of otherwise normal myocardial function. Severe thiamine deficiency (Beriberi), in which buildup of pyruvate and lactate in the blood leads to systemic vasodilation, also results in a high CO state and cardiomyopathy. Low SVR and high-output failure may also be secondary to many other conditions, including arteriovenous malformation, liver disease, myeloproliferative disorders, acromegaly, and Paget disease of bone, but associated clinical features distinguish them from CS.²⁹ High-output states are commonly detrimental to right heart structures and function, but in the few subjects with CS, in which RV function was assessed, this was not apparent. High-output cardiac hypertrophy in CS may compete in differential diagnosis for HF with preserved ejection fraction. However, HF with preserved ejection fraction is essentially a diastolic HF condition, whereas diastolic function is essentially normal in CS.

Athlete's heart syndrome, associated with eccentric enlargement as a consequence of repetitive cardiac

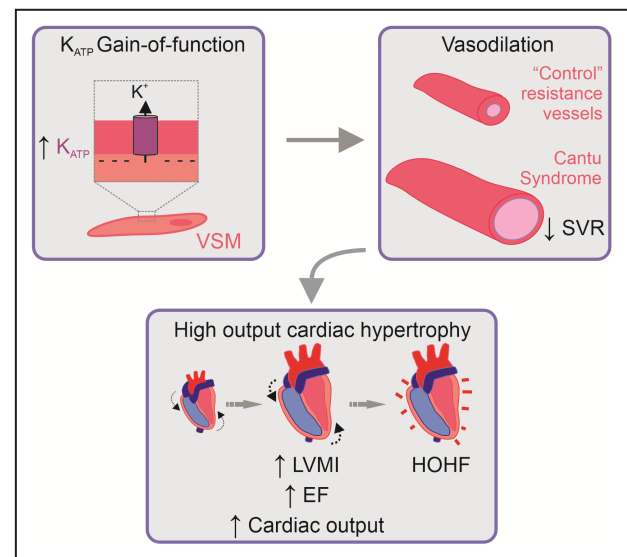


Figure 6. Mechanism of cardiovascular pathophysiology in CS.

(Top left) K_{ATP} channel composed of Kir6.1 (*KCNJ8*) and SUR2 (*ABCC9*) is expressed in the plasma membrane of smooth muscle cells, including VSM. CS-associated *ABCC9* or *KCNJ8* variants cause gain-of-function of K_{ATP} channels in VSM, driving hyperpolarization of the membrane potential. (Top right) VSM membrane potential hyperpolarization is predicted to result in chronic vasodilation in CS, as reflected by marked decreases in SVR. (Bottom) Cardiac remodeling to high-output hypertrophic state arises secondary to chronically lowered SVR, resulting in elevated cardiac mass, contractility, and output in subjects with CS. This progresses to HOHF in older subjects. CS indicates Cantu syndrome; EF, ejection fraction; HOHF, high-output heart failure; K_{ATP} , ATP-sensitive potassium; LVMI, left ventricular mass index; SVR, systemic vascular resistance; and VSM, vascular smooth muscle.

loading,³⁰ is a superficially similar cardiac phenotype. Notably, athlete's heart syndrome is generally considered benign, without physical symptoms, other than persistently low resting heart rate.³¹ CS is associated with additional cardiovascular issues that are not present in athlete's heart syndrome, but which could also feature in other high-output hypertrophic states. Features of fetal circulation, such as persistent PDA and dilated and tortuous collateral arteries in general, are common findings in subjects with CS,^{32,33} and are consistent with the proposed basis of the cardiac phenotype as a response to decreased SVR.

CS thus represents a sentinel example of a secondary cardiac condition that could, in principle, arise from a primary abnormal vasodilation of any cause. The long-term prognosis of this high-output cardiac hypertrophy is not clear. Interestingly, in the only large-scale analysis of subjects with high-output HF of various causes, both high output and mortality were strongly correlated with the severity of decreased SVR, and outcomes were poorest among subjects with the lowest SVR.²⁹ These findings do suggest that low SVR and the consequent

high-output hypertrophic cardiac response may not be benign. We would predict that the condition should be associated with a decreased reserve in terms of ability to respond to additional demands, and the 7 years of our systematic study reveal a trend toward worsening clinical HF status. Additionally, 4 of the 5 subjects who were aged >40 years, all women, showed signs of high-output HF. High-output HF^{29,34} exhibits similar features to the cardiovascular phenotype in CS (including decreased exercise tolerance, low SVR, and elevated CO). CS may therefore represent a genetically defined basis for high-output HF.

A full understanding of the long-term cardiovascular manifestations of CS, facilitated by recognition of the underlying molecular cause, may have clearer significance for potential therapeutic approaches. Because of the current lack of awareness of CS complications, many subjects with CS have been misdiagnosed with hypertrophic cardiomyopathy or dilated cardiomyopathy, and as a result have been administered conventional therapies including angiotensin-converting enzyme inhibitors or other vasodilatory agents, diuretics, β -blockers, or sildenafil.⁹ Treatment with these agents are based on HF paradigms that do not take into account low SVR states and will exacerbate the underlying primary decrease in SVR and hence worsen symptoms. Ultimately, an appropriate therapy for CS, and potentially for other causes of high-output cardiac hypertrophy caused by decreased SVR, will address the underlying primary vasorelaxation. In the specific case of CS, this might ideally be a blocker of the overactive K_{ATP} channels themselves. Animal studies have shown that the K_{ATP} channel inhibitor glibenclamide reverses the primary decrease in SVR, and hence the secondary cardiac enlargement,³⁵ raising the possibility that this approach may be effective, by treating the underlying defect directly.

Limitations of the Study

CS is rare and underdiagnosed, limiting the available sample size for this study. Presentation of the characteristic cardiac phenotype and natural history may help improve diagnosis of CS, and identification of the relevant cardiac features. In the majority of cases, hemodynamics were primarily determined by noninvasive tests rather than by cardiac catheterization. However, limited validation in a few subjects with CS confirmed the accuracy of noninvasive-derived hemodynamic data.

ARTICLE INFORMATION

Received August 19, 2022; accepted October 25, 2022.

Affiliations

Division of Cardiology, Department of Pediatrics (G.K.S., M.A.); Center for the Investigation of Membrane Excitability Diseases (CIMED) (G.K.S., C.M., M.S.R., D.K.G., C.G.N.); Department of Cell Biology and Physiology (C.M.,

C.G.N.); Division of Statistics (H.G.); Department of Medicine, Division of Endocrinology (M.S.R.) and Department of Pediatrics, Division of Genetics, Washington University School of Medicine, St. Louis, MO (D.K.G.).

Acknowledgments

The authors thank the subjects and families for their participation and consent to publish this work, and the many volunteers who have helped to make the Cantu syndrome research clinic happen. Clinical assessments were performed by G.K.S., M.A., and D.K.G. Research clinic activities were coordinated by D.K.G., M.A., M.S.R., G.K.S., and C.G.N. The registry was developed by D.K.G., G.K.S., C.M., and C.G.N. Data analysis was performed by G.K.S., H.G., C.M., and C.G.N. The article was written by G.K.S., C.M., and C.G.N., and edited by the other authors.

Sources of Funding

This work was supported in part by National Institutes of Health grants R21 HD103347 (Eunice Kennedy Shriver National Institute of Child Health & Human Development to D.K.G. and C.G.N.) K99 HL150277 and R35 HL140024 (National Heart, Lung, and Blood Institute to C.G.N. and C.M.), and the Children's Discovery Institute (CH-MD-II-2015-488 to C.G.N.) and the Center for the Investigation of Membrane Excitability Diseases Pilot and Feasibility program (CIMED-14-03 to D.K.G.). C. McClenaghan is supported by a National Institutes of Health grant K99 HL150277.

Disclosures

None.

REFERENCES

- Hunt SA, Abraham WT, Chin MH, Feldman AM, Francis GS, Ganiats TG, Jessup M, Konstam MA, Mancini DM, Michl K, et al. 2009 focused update incorporated into the ACC/AHA 2005 guidelines for the diagnosis and management of heart failure in adults: a report of the American College of Cardiology Foundation/American Heart Association Task Force on Practice Guidelines: developed in collaboration with the International Society for Heart and Lung Transplantation. *Circulation*. 2009;119:e391–e479. doi: 10.1161/CIRCULATIONAHA.109.192065
- Marketou ME, Parthenakis F, Vardas PE. Pathological left ventricular hypertrophy and stem cells: current evidence and new perspectives. *Stem Cells Int*. 2016;2016:5720758. doi: 10.1155/2016/5720758
- Brownstein CA, Towne MC, Luquette LJ, Harris DJ, Marinakis NS, Meinecke P, Kutsche K, Campeau PM, Yu TW, Margulies DM, et al. Mutation of KCNJ8 in a patient with Cantu syndrome with unique vascular abnormalities—support for the role of K(ATP) channels in this condition. *Eur J Med Genet*. 2013;56:678–682. doi: 10.1016/j.ejmg.2013.09.009
- Cooper PE, Reutter H, Woelfle J, Engels H, Grange DK, van Haften G, van Bon BW, Hoischen A, Nichols CG. Cantu syndrome resulting from activating mutation in the KCNJ8 gene. *Hum Mutat*. 2014;35:809–813. doi: 10.1002/humu.22555
- Harakalova M, van Harssel JJ, Terhal PA, van Lieshout S, Duran K, Renkens I, Amor DJ, Wilson LC, Kirk EP, Turner CL, et al. Dominant missense mutations in ABCC9 cause Cantu syndrome. *Nat Genet*. 2012;44:793–796. doi: 10.1038/ng.2324
- van Bon BW, Gilissen C, Grange DK, Hennekam RC, Kayserili H, Engels H, Reutter H, Ostergaard JR, Morava E, Tsiakas K, et al. Cantu syndrome is caused by mutations in ABCC9. *Am J Hum Genet*. 2012;90:1094–1101. doi: 10.1016/j.ajhg.2012.04.014
- Grange DK, Lorch SM, Cole PL, Singh GK. Cantu syndrome in a woman and her two daughters: further confirmation of autosomal dominant inheritance and review of the cardiac manifestations. *Am J Med Genet A*. 2006;140:1673–1680. doi: 10.1002/ajmg.a.31348
- Scurr I, Wilson L, Lees M, Robertson S, Kirk E, Turner A, Morton J, Kidd A, Shashi V, Stanley C, et al. Cantu syndrome: report of nine new cases and expansion of the clinical phenotype. *Am J Med Genet A*. 2011;155A:508–518. doi: 10.1002/ajmg.a.33885
- Grange DK, Roessler HI, McClenaghan C, Duran K, Shields K, Remedi MS, Knoers N, Lee JM, Kirk EP, Scurr I, et al. Cantu syndrome: findings from 74 patients in the International Cantu Syndrome Registry. *Am J Med Genet C Semin Med Genet*. 2019;181:658–681. doi: 10.1002/ajmg.c.31753
- Levin MD, Zhang H, Uchida K, Grange DK, Singh GK, Nichols CG. Electrophysiologic consequences of KATP gain of function in the heart: conduction abnormalities in Cantu syndrome. *Heart Rhythm*. 2015;12:2316–2324. doi: 10.1016/j.hrthm.2015.06.042

11. Levin MD, Singh GK, Zhang HX, Uchida K, Kozel BA, Stein PK, Kovacs A, Westenbroek RE, Catterall WA, Grange DK, et al. KATP channel gain-of-function leads to increased myocardial L-type Ca²⁺ current and contractility in Cantu syndrome. *Proc Natl Acad Sci USA*. 2016;113:6773–6778. doi: 10.1073/pnas.1606465113
12. Flynn JT. High blood pressure in the young: why should we care? *Acta Paediatr*. 2018;107:14–19. doi: 10.1111/apa.14110
13. Lang RM, Mor-Avi V, Sugeng L, Nieman PS, Sahn DJ. Three-dimensional echocardiography: the benefits of the additional dimension. *J Am Coll Cardiol*. 2006;48:2053–2069. doi: 10.1016/j.jacc.2006.07.047
14. Devereux RB, Alonso DR, Lutas EM, Gottlieb GJ, Campo E, Sachs I, Reichek N. Echocardiographic assessment of left ventricular hypertrophy: comparison to necropsy findings. *Am J Cardiol*. 1986;57:450–458. doi: 10.1016/0002-9149(86)90771-X
15. Khoury PR, Mitsnefes M, Daniels SR, Kimball TR. Age-specific reference intervals for indexed left ventricular mass in children. *J Am Soc Echocardiogr*. 2009;22:709–714. doi: 10.1016/j.echo.2009.03.003
16. Daniels SR, Loggie JM, Khoury P, Kimball TR. Left ventricular geometry and severe left ventricular hypertrophy in children and adolescents with essential hypertension. *Circulation*. 1998;97:1907–1911. doi: 10.1161/01.CIR.97.19.1907
17. Lang RM, Bierig M, Devereux RB, Flachskampf FA, Foster E, Pellikka PA, Picard MH, Roman MJ, Seward J, Shanewise J, et al. Recommendations for chamber quantification. *Eur J Echocardiogr*. 2006;7:79–108. doi: 10.1016/j.euje.2005.12.014
18. Greenberg NL, Firstenberg MS, Castro PL, Main M, Travaglini A, Odabashian JA, Drinko JK, Rodriguez LL, Thomas JD, Garcia MJ. Doppler-derived myocardial systolic strain rate is a strong index of left ventricular contractility. *Circulation*. 2002;105:99–105. doi: 10.1161/hc0102.101396
19. Nagueh SF, Middleton KJ, Kopelen HA, Zoghbi WA, Quinones MA. Doppler tissue imaging: a noninvasive technique for evaluation of left ventricular relaxation and estimation of filling pressures. *J Am Coll Cardiol*. 1997;30:1527–1533. doi: 10.1016/S0735-1097(97)00344-6
20. Eidem BW, McMahon CJ, Cohen RR, Wu J, Finkelshteyn I, Kovalchin JP, Ayres NA, Bezold LJ, O'Brian Smith E, Pignatelli RH. Impact of cardiac growth on Doppler tissue imaging velocities: a study in healthy children. *J Am Soc Echocardiogr*. 2004;17:212–221. doi: 10.1016/j.echo.2003.12.005
21. Dabestani A, Mahan G, Gardin JM, Takenaka K, Burn C, Allfie A, Henry WL. Evaluation of pulmonary artery pressure and resistance by pulsed Doppler echocardiography. *Am J Cardiol*. 1987;59:662–668. doi: 10.1016/0002-9149(87)91189-1
22. Kitabatake A, Inoue M, Asao M, Masuyama T, Tanouchi J, Morita T, Mishima M, Uematsu M, Shimazu T, Hori M, et al. Noninvasive evaluation of pulmonary hypertension by a pulsed Doppler technique. *Circulation*. 1983;68:302–309. doi: 10.1161/01.CIR.68.2.302
23. Levy PT, Patel MD, Groh G, Choudhry S, Murphy J, Holland MR, Hamvas A, Grady MR, Singh GK. Pulmonary artery acceleration time provides a reliable estimate of invasive pulmonary hemodynamics in children. *J Am Soc Echocardiogr*. 2016;29:1056–1065. doi: 10.1016/j.echo.2016.08.013
24. Gamble G, Zorn J, Sanders G, MacMahon S, Sharpe N. Estimation of arterial stiffness, compliance, and distensibility from M-mode ultrasound measurements of the common carotid artery. *Stroke*. 1994;25:11–16. doi: 10.1161/01.STR.25.1.11
25. Flagg TP, Kurata HT, Masia R, Caputa G, Magnuson MA, Lefer DJ, Coetzee WA, Nichols CG. Differential structure of atrial and ventricular KATP: atrial KATP channels require SUR1. *Circ Res*. 2008;103:1458–1465. doi: 10.1161/CIRCRESAHA.108.178186
26. McClenaghan C, Huang Y, Matkovich SJ, Kovacs A, Weinheimer CJ, Perez R, Broekelmann TJ, Harter TM, Lee JM, Remedi MS, et al. The mechanism of high-output cardiac hypertrophy arising from potassium channel-of-function in Cantu syndrome. *Function (Oxf)*. 2020;1:zqaa004.
27. Huang Y, McClenaghan C, Harter TM, Hinman K, Halabi CM, Matkovich SJ, Zhang H, Brown GS, Mecham RP, England SK, et al. Cardiovascular consequences of KATP overactivity in Cantu syndrome. *JCI Insight*. 2018;3:e121153.
28. Menon SC, Eidem BW, Dearani JA, Ommen SR, Ackerman MJ, Miller D. Diastolic dysfunction and its histopathological correlation in obstructive hypertrophic cardiomyopathy in children and adolescents. *J Am Soc Echocardiogr*. 2009;22:1327–1334. doi: 10.1016/j.echo.2009.08.014
29. Reddy YNV, Melenovsky V, Redfield MM, Nishimura RA, Borlaug BA. High-output heart failure: a 15-year experience. *J Am Coll Cardiol*. 2016;68:473–482. doi: 10.1016/j.jacc.2016.05.043
30. Beaumont A, Hough J, Sculthorpe N, Richards J. Left ventricular twist mechanics during incremental cycling and knee extension exercise in healthy men. *Eur J Appl Physiol*. 2017;117:139–150. doi: 10.1007/s00421-016-3506-8
31. Doyen B, Matelot D, Carre F. Asymptomatic bradycardia amongst endurance athletes. *Phys Sportsmed*. 2019;47:249–252. doi: 10.1080/00913847.2019.1568769
32. Leon Guerrero CR, Pathak S, Grange DK, Singh GK, Nichols CG, Lee JM, Vo KD. Neurologic and neuroimaging manifestations of Cantu syndrome: a case series. *Neurology*. 2016;87:270–276. doi: 10.1212/WNL.0000000000002861
33. Hiraki Y, Miyatake S, Hayashidani M, Nishimura Y, Matsuura H, Kamada M, Kawagoe T, Yunoki K, Okamoto N, Yofune H, et al. Aortic aneurysm and craniosynostosis in a family with Cantu syndrome. *Am J Med Genet A*. 2014;164A:231–236. doi: 10.1002/ajmg.a.36228
34. Mehta PA, Dubrey SW. High output heart failure. *QJM*. 2009;102:235–241. doi: 10.1093/qjmed/hcn147
35. McClenaghan C, Huang Y, Yan Z, Harter TM, Halabi CM, Chalk R, Kovacs A, van Haaften G, Remedi MS, Nichols CG. Glibenclamide reverses cardiovascular abnormalities of Cantu syndrome driven by KATP channel overactivity. *J Clin Invest*. 2020;130:1116–1121. doi: 10.1172/JCI130571